Flavonoid Glycosides from *Persea caerulea*. Unraveling their interactions with SDS-Micelles through Matrix-Assisted DOSY, PGSE, Mass spectrometry and NOESY.

Juan M. Álvarez,[†,‡] Álvaro Raya-Barón,[§] Pedro M. Nieto,[#] Luis E. Cuca,[†] Alegría Carrasco,[‖] Alberto Fernández-Gutiérrez,[‖] Ignacio Fernández*[§,⊧]*

† Department of Chemistry, Universidad Nacional de Colombia, Bogota, E-111321 (Colombia).

‡ Department of Chemistry, Universidad del Magdalena, Santa Marta, E-470003 (Colombia).

§ Department of Chemistry and Physics, ceiA3, Universidad de Almería, Almería, E-04120 (Spain).

Glycosystems Laboratory, Department of Bioorganic Chemistry, Instituto de Investigaciones Químicas (CSIC - US), cicCartuja, Americo Vespucio, 49, Sevilla, E-41092 (Spain).

‖ Department of Analytical Chemistry, Universidad de Granada, Granada, E-18001 (Spain).

⊧ BITAL, Research Centre for Agricultural and Food Biotechnology, Almería (Spain).

KEYWORDS. *Persea caerulea,* flavonoid glycosides, Matrix-Assisted DOSY, inter-proton distances, micelles.

ABSTRACT. Two flavonide glycosides derived from rhamnopyranoside (**1**) and arabinofuranoside (**2**), have been isolated from leaves of *Persea caerulea* for the first time. The structures of **1** and **2** have been established by ^{1}H NMR, ^{13}C NMR and IR spectroscopy, together with LC-ESI-TOF and LC-ESI-IT MS spectrometry. From the MS and MS/MS data, the molecular weights of the intact molecules as well as those of quercetin and kaempferol together with their sugar moieties were deduced. The NMR data provided information on the identity of the compounds, as well as the α and β configurations and the position of the glycosides on quercetin and kaempferol. We have also explored the application of sodium dodecyl sulfate (SDS) normal micelles in binary aqueous solution, at a range of concentrations, to the diffusion resolution of these two glycosides, by the application of matrix-assisted DOSY (MAD) and PGSE methodologies, showing that SDS micelles offer a significant resolution which can, in part, be rationalized in terms of differing degrees of hydrophobicity, amphiphilicity and steric effects. In addition, intra- and inter-residue proton−proton distances using NOE build-up curves were used to elucidate the conformational preferences of these two flavonoid glycosides when interacting with the micelles. By the combination of both diffusion and NOESY techniques, the average location site of kaempferol and quercetin glycosides has been postulated, with the former exhibiting a clear insertion into the interior of the SDS-micelle, whereas the latter is placed closer to the surface.

INTRODUCTION

Flavonoids are plant secondary metabolites which bear a diphenylpropane moiety as the main structural feature. They are widely distributed in nature and are usually found in fruits and vegetables mainly as glycosides in vacuoles.[1] In different environmental conditions they are secreted, if necessary hydrolyzed, or transported to different organelles or tissues/organs. All flavonoid glycosides have a C15 phenyl-benzopyrone skeleton to which glycosidic moieties are attached via either an O atom (–O–) or a skeletal C atom (–C–).[2] These classes of secondary metabolites play an important role in the interactions of plants with their environment.[3] Flavonoid glycosides and free aglycones are involved in the interactions of plants with microorganisms, whether pathogenic and symbiotic.[4,5,6] Their activity in humans have been the subject of extensive research and they have been reported to exhibit numerous biological activities such as antioxidant, anti-inflammatory, oestrogenic, cytotoxic antitumoral, antiviral and many others.[7] The flavonoids under study in the current research, kaempferol-3-O-rhamnopyranoside **1** and quercetin-3-O-arabinofuranoside **2** have been isolated from different plant species.[8,9,10] In the genus *Persea*, **1** is herewith reported by first time for *P. caerulea*, but has been previously isolated from P. americana leaves, exhibiting antiviral activity against acyclovir-HSV1.[11,12] As far as quercetin-3-O-α-L-arabinofuranoside **2** is concerned, there are no previous reports, describing its presence in the genus *Persea*. This species is characterized for its anti-inflammatory properties and anti-infective effects.[13] It is worth mentioning that rapid and reliable methods for the analysis and identification of these natural polyphenolic compounds is therefore of remarkable importance. Liquid chromatography coupled to mass spectrometry (LC-MS) represents a very powerful tool for their analysis,[14,15] although, as it will be seen here, some other techniques can be also used for elucidating not only their structure but also their

interactions with supramolecular systems such as micelles. Very recently, Pichette and coworkers have employed ROESY NMR and DFT calculations to ascertain the chemical structure of non-caretonoid abibalsamins isolated from *Abies balsamea,* although no other techniques such as Diffusion NMR and NOESY build-up curves were employed.[16]

RESULTS AND DISCUSSION

Two flavonoid glycosides kaepmferol-3-O-α-L-rhamnopyranoside (**1**) and quercetin-3-O-α-L-arabinofura (**2**) have been isolated from the ethanolic extract of the leaves of *P. caerulea* for the first time. Inspired by the work of Morris and coworkers[17] we have investigated their interactions with sodium dodecyl (SDS) micelles in binary solvent mixtures. We have elucidated critical interactions that allowed the separation of their NMR signals efficiently through the use of PGSE and DOSY methodologies, and determined the place and strength of their distinct intermolecular contacts through NOESY build-up curves and DFT calculations.

Compounds **1** and **2** are glycosides substituted at C-3 with free hydroxyl groups at C-5 and C-7 as indicated in Scheme 1.

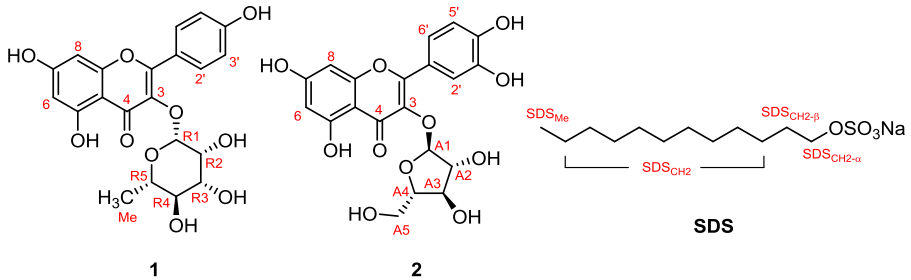

Scheme 1. Chemical structures and labels of **1**, **2** and sodium dodecyl sulfate dodecyl SDS.

Anomeric configurations, location and type of sugar in the flavonoid glycosides can be determined using some NMR information, such as ^{1}H NMR chemical shifts, vicinal and geminal

coupling constants, ^{13}C NMR chemical shifts, ^{1}H-^{1}H coupling constants, long-range homo- and heteronuclear correlations and inter-residue NOE. The anomeric resonances of α-glycosides usually resonate 0.3-0.5 ppm to higher frequency compared with that of the corresponding β-glycosides due to ring and C-C diamagnetic anisotropy effects. Thus, resonances at 4.5-5.5 ppm, which are doublets with 1-4 Hz coupling, are of α-anomeric protons, whereas doublets with 6-8 Hz appear between 4.0 and 4.8 ppm belong to β-anomeric protons as is expected for monosaccharides stereochemistry.[18]

Compounds **1** and **2** are shown to be kaepmferol-3-O-α-L-rhamnopyranoside and quercetin-3-O-α-L-arabinofuranoside, respectively using the ^{1}H, ^{13}C, DEPT NMR, ^{1}H-^{1}H COSY, ^{1}H-^{1}H TOCSY, ^{1}H-^{13}C HMQC and ^{1}H-^{13}C HMBC spectral data (see Table 1 and Supporting Information). To the best of our knowledge, this is the first report on the occurrence of these two flavonoid glycosides in this *Persea caerulea* leaves.

The identity of the flavonol moiety in **1** and **2** was first confirmed by comparison of NMR spectra with published chemical shifts for kaempferol and quercetin.[18,19] The glycosidic nature of the flavonoids is evidenced by the observation of several resonances typical of sugar moieties. The linkage position of the flavonoid, the sugar identity and the *alpha* or *beta* configuration is usually derived from comparison with reference compounds. Typically a sugar moiety on the 3-hydroxyl group of, for instance, quercetin, would cause only very minor variations on chemical shifts on H5′, H6, H8 and slightly larger shifts on H2′ and H6′, whereas sugar moieties at other positions would modify to different extents these chemical shifts and also their multiplicities.[20] In addition, the mass of the sugar moiety can be calculated from the difference in mass between the molecular ion and some fragment ions. As will be discussed below, from the MS results (Table 2) we conclude that both glycosidic moieties were monosaccharides.

Table 1. ^{1}H and ^{13}C NMR Data (chemical shifts) of compounds **1** and **2**.[a]

Entry	δ_C	δ_H	δ_C	δ_H
	Flavonoid glycoside **1**		Flavonoid glycoside **2**	
2	158.0		158.0	
3	135.7		134.4	
4	179.3		179.8	
5	163.2	12.72, OH, s	163	12.5, OH, s
6	99.5	6.27, d (2.1)	99.6	6.28, d (2.1)
7	164.9	9.69, OH, s	165.2	9.76, OH, s
8	94.5	6.49, d (2.1)	94.6	6.52, d (2.1)
9	158.4		157.9	
10	105.8		105.4	
1’	122.5		122.7	
2’	131.6	7.86, 2H, d, (8.8)	116.6	7.74, d (2.1)
3’	116.4	7.02, 2H, d (8.8)	149.3	8.57, OH, s
4’	160.9	9.11, OH, s		
5’			116.3	7.00, d (8.4)
6’			122.4	7.57, dd (2.1, 8.4)
A,R-1	102.6	5.54, d (1.4)	109.1	5.49, s
A,R-2	71.5	4.23, dt (3.8, 1.8), 4.16, OH, d (3.8)	82.3	4.31, dd (7.1, 1.6), 4.8, OH, d (7.1)
A,R-3	72.1	3.71, m	78.9	3.99, ddd (8.5, 3.1, 1.7), 4.88, OH, d (8.5)
A,R-4	71.3	3.33, m, 3.86, OH, m	89.4	4.11, c (3.7)
A,R-5	73	3.30, m	62.7	3.60, 2H, t (4.4), 4.38, OH, t (4.4)
R-Me	16.9	0.90, d (5.9)		

[a] Spectra were recorded at both 300 MHz and 500 MHz spectrometers. Compounds **1** and **2** were measured in Me_2CO-d_6. Coupling constants are (*J* in Hz) in parenthesis.

The type of monosaccharide moietys usually found in nature are glucose, galactose, xylose, rhamnose, arabinose, mannose, allose, apiose, galacturonic acid, and glucoronic acid.[21] As mentioned above, the combined use of literature and own MS data, showed that compounds **1** and **2** contained rhamnose and arabinose units, respectively.

The molar ratio between **1** and **2** was established from the integration of the well-resolved anomeric proton signals of both compounds in the ^{1}H NMR spectrum located at δ_H 5.54 and 5.49 ppm for **1** and **2**, respectively. Their relative integral established a ratio of 0.4:1.0 for **1** and **2**, respectively. Compound **1** and **2** were confirmed after the complete interpretation of the NMR data and the comparison with data reported in the literature regarding **1**[19,22,23] and **2**.[19,20,22,24,25,26,27,28] In the Supporting Information (Tables S1 and S2) one could find a detailed comparison of previously reported data with the data described herein.

Regarding the LC-MS analysis of **1** and **2**; the negative ESI-TOF mass spectrum of **1** showed a pseudo-molecular ion at *m/z* 431.0990 $[M-H]^-$ corresponding to the formula $C_{21}H_{19}O_{10}$ with an absolute error in ppm of 2.8 and an isotopic pattern fit factor (mSigma) of 12 (see Experimental Section). An aglycone ion peak at m/z 284.7 and another ion peak at *m/z* 254.8 were also found, corroborating the NMR assignment for kaepmferol-3-O-α-L-rhamnopyranoside **1**. For compound **2**, the accurate ESI-TOF MS spectrum showed a pseudo-molecular ion $[M-H]^-$ at *m/z* 433.0781 as the predominant signal, corresponding to the formula $C_{20}H_{17}O_{11}$. In this case, the absolute error in ppm was 2.3 and an isotopic pattern fit factor (mSigma) value of 21 (see Experimental Section). The ion peak at m/z 300.7 confirmed the assignment and establishes the molecule to be quercetin-3-O-α-L-arabinofuranoside **2**.

Table 2. LC-ESI-TOF MS and LC-ESI-IT MS results for kaepmferol-3-O-α-L-rhamnopyranoside **1** and quercetin-3-O-a-L-arabinofuranoside **2** detected in the ethanolic extract of *P. caerulea*. In brackets are shown m/z theoretical values for both compounds.

Pseudo-MF[b]	$C_{21}H_{19}O_{10}$ (**1**)[a]	$C_{20}H_{17}O_{11}$ (**2**)[a]
LC-ESI-TOF MS (NP)	431.0990 (431.0978)	433.0781 (433.0771)
LC-ESI-IT MS		
$[M+H]^+$	432.9	434.9
$[M-H]^-$	430.9	432.9
MS/MS (NP)	284.7; 254.8	300.7

[a] At the optimum chromatographic conditions, the retention times were 10.2 and 9.0 min, respectively, for kaepmferol-3-O-α-L-rhamnopyranoside **1** and quercetin-3-O-α-L-arabinofuranoside **2**. [b] Pseudo molecular formula corresponding to the accurate $[M-H]^-$.

O-glycoside flavonoids can be distinguished by their positive or negative ionization spectra.[29] For this type of metabolite, the application of low or medium fragmentation energy results in heterolytic cleavage of their hemi-acetal O–C bonds, yielding distinctive fragments.[30,31] In the current study, the MS/MS signals coming from **1** lead to the following fragments: one fragment of *m/z* 284.7, characteristic of the flavonoid aglycon of kaempferol, and another one of *m/z* 254, produced by the loss of a 30 unit of CH_2O. The latter is also characteristic of this type of flavonoid (Scheme 2a). In the case of **2**, a predominant MS fragment at *m/z* 300.7 was observed, corresponding to quercetin (Scheme 2b). It was observed a loss of 146 Da for **1**, which was indicative of the elimination of the sugar unit as a deoxy-hexose sugar, corresponding to rhamnose.

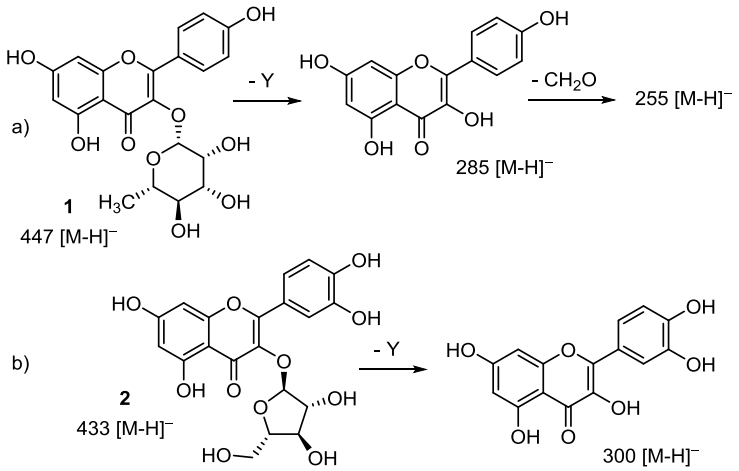

Scheme 2. Proposed fragmentation pathway for a) kaempferol -3-O-rhamnopyranoside **1**, and b) quercetin-3-O-arabinofuranoside **2**.

As far as **2** is concerned, the elimination of a 132 unit, corresponded to the sugar unit as a pentose sugar,[28] which provides the fragment of m/z at 300.7, clearly observed in the mass spectrum (Scheme 2b). The IR spectrum for the mixture of compounds showed hydroxyl absorptions at 3700-3300 cm^{-1}, bands at 1600 and 1660 cm^{-1} due to the presence of an α,β-unsaturated carboxyl function, other peaks at 2930 cm^{-1} due to methine and methylene groups, and peaks at 1500-1600 cm^{-1} due to combinations bands for aromatic rings. These data confirm the presence of the functional groups of the flavonoid glycosides **1** and **2** and corroborate with the NMR and MS/MS assignments.

Diffusion studies. Although we could characterize both compounds in the mixture thanks to the strength and robustness of NMR techniques, we were interested in the study of their diffusion properties through PGSE and Diffusion Ordered Spectroscopy (DOSY), important tools used nowadays in the analysis of mixtures.[32] It is important to mention that diffusion NMR methods usually fails when diffusion coefficients and therefore sizes are very similar, or when there are spectra with extensive signal overlap.[33] Recently, it has been shown that performing DOSY in a

matrix with which the analytes interact differentially can resolve signals from compounds with similar diffusion behavior. In such a matrix-assisted DOSY (MAD) experiment the interaction of the analytes with the matrix drives the average diffusion coefficients. The effective diffusion coefficient under these conditions may differ greatly from its solution value when the analyte is present, and therefore the goal is signal differentiation and not quantification of the diffusion coefficient (D-value). Such behavior of the various solutes in the NMR technique closely parallels their behavior in liquid chromatography and therefore is also widely known as NMR ‘‘chromatography”.[34] Enhanced resolution in DOSY spectra was achieved for the first time by Morris and coworkers by addition of micelles, in the case of hydrophobic interactions.[35] As mentioned above, Morris and coworkers reported for the first time an efficient methodology for NMR analysis of flavonoids using SDS to separate the NMR signals of compounds of similar size such as flavone, fisetin, (+)-catechin and quercetin.[17] This method has been also extended to high-resolution magic angle spinning (HRMAS) NMR where the use of silica gel has been used to achieve well-separated and high-resolution spectra for the single components.[36]

In recent years, it has been shown that micelles, both normal and reverse, can be used as separation agents to distinguish between the isomers of dihydroxybenzene, catechol, resorcinol and hydroquinone, in DOSY experiments,[37] between the isomers of methoxyphenol,[38] and also in the differentiation of medium chain length alcohols.[39] Other resolving agents for diffusion NMR have been employed in liquid NMR such as polyvinylpyrrolidone (PVP),[40] polyethyleneglycol,[41] and silica gel,[42] the latter finding satisfactorily results when matching the magnetic susceptibilities of both solvent and type of silica. Chiral versions have been also achieved by the use of β-cyclodextrins, allowing the resolution of a mixture of two native epimers.[43] More recently, Nilsson and coworkers have presented the use of Brij nonionic

surfactant in mixed solvents for the DOSY analysis of mixtures relevant to natural products.[44] Finally, the use of nanostructured dispersed media, such as microemulsions, have found also application for the separation of complex mixtures.[45]

To the best of our knowledge the challenge to apply MAD and PGSE methods to flavonoid glycosides with high structural similarity has never been achieved, and is therefore the problem we face herein by the use of surfactants-based micelles such as those form with sodium dodecyl sulfate (SDS). It is well known that surfactants in water spontaneously self-assemble to form micelles where the factors influencing their formation in terms of size and shape have been the subject of a plethora of studies in the last decades.[46] The presence of SDS as well defined micelles in binary solvent mixtures such as water-DMSO has been confirmed previously by investigating the dependence of the diffusion coefficients as a function of SDS concentration,[17] showing that the critical micelle concentration (CMC) changed from 7 mM (pure D_2O) to 11 mM (20% v/v DMSO-d_6) or 25 mM (50% DMSO-d_6), consistent with other literature.[47] Interestingly, Hoffmann *et al*. have studied the interactions of toluene and cyclohexane with SDS as a new tool for the structural elucidation of microemulsions.[48]

DOSY plots and PGSE signal attenuations are shown in Figure 1 for the mixture of flavonoid glycosides **1** and **2** in Me_2CO-d_6 at room temperature. As can be observed, their diffusion coefficients (and therefore their hydrodynamic radii), are too similar for their signals to be separable, suggesting the need for a matrix-assisted experiment. Often the Stokes-Einstein equation[49] and its modifications[50] are useful and enable molecular size estimation of large particles that are much larger than the solvent. These calculated hydrodynamic radii, r_H, assume spherical shapes; hence, they do not represent the real shape of the molecules. Nevertheless, their use is well established for comparisons, since they offer a rapid and easy method to recognize

ion pairing and/or aggregation. As it is shown in Table 3, adding SDS to the mixture of compounds completely changed the situation. Several diffusion experiments were performed using SDS from 25 to 180 mM, and showed due to their different interaction with the micelles, that the diffusion coefficient of **1** is readily separated from that of **2**, being this difference more pronounced within increasing the concentration of SDS (entries 16 and 17, Table 3).

In simple acetone solution (Figure 1a) the two flavonoids derivatives have almost the same diffusion coefficient (11.1 10^{-10} m^2 s^{-1}) with no difference in their hydrodynamic radii (Δr_H = -0.04 Å).

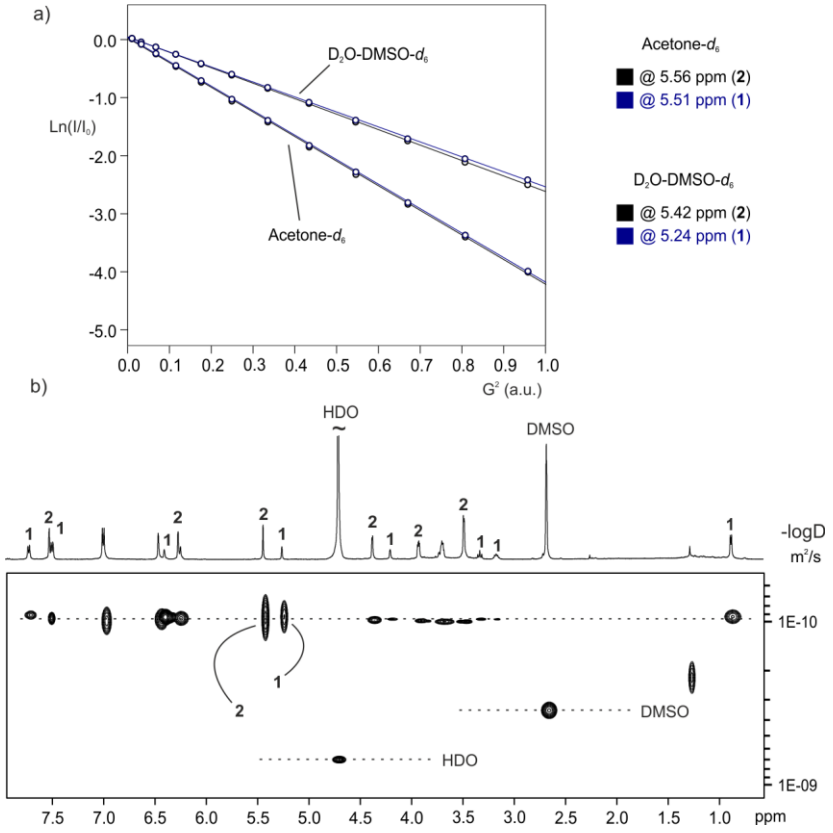

Figure 1. a) Linearized Stejskal−Tanner fit of the PGSE NMR data for **1** and **2** in both Me_2CO-d_6 and a binary mixture based on DMSO-d_6-D_2O (20% v/v). b) ^1H DOSY (500 MHz) spectrum with the least attenuated 1D spectrum on top, for a sample containing no SDS in DMSO-d_6-D_2O (20 % v/v) at room temperature.

Table 3. Diffusion coefficient (*D*) and Stokes-Einstein hydrodynamic radius (r_H) values for compounds **1** and **2** at room temperature in DMSO-d_6-D_2O (20% v/v) as a function of SDS concentration.

SDS (mM)	Comp.	$D \times 10^{-10}$ (m^2 s^{-1})[a]	ΔD (**1**-**2**)	r_H (Å)[b]	Δr_H (**1**-**2**)
	1[c]	11.131		6.23	
	2[c]	11.074	-0.0057	6.27	-0.04
	1[d]	1.005		10.34	
	2[e]	1.036	0.00313	10.04	0.3
	HDO[f]	6.915		1.50	
	DMSO[g]	3.703		2.81	
25	**1**	0.8578		12.13	
	2	0.9211	0.00633	11.29	0.84
	SDS	0.8055		12.9	
60	**1**	0.8544		12.18	
	2	0.9267	0.00723	11.21	0.97
	SDS	0.8095		12.90	
120	**1**	0.7644		13.61	
	2	0.8546	0.00902	12.18	1.43
	SDS	0.6200		16.80	
180	**1**	0.6849		15.20	
	2	0.8226	0.01377	12.64	2.56
	SDS	0.5095		20.40	
	HDO[f]	6.742		1.54	
	DMSO[g]	3.607		2.88	

[a] The experimental error in the *D* values is ±2 %. [b] The viscosities used in the Stokes-Einstein equation were taken from Perry's Chemical Engineers' Handbook 8th Edition and were 0.3147 and 0.2077 10^{-3} Kg s^{-1} m^{-1} for acetone and dimethylsulfoxide, respectively. [c] In Me_2CO-d_6. [d] The

signal at δ_H 5.24 ppm was monitored. [e] The signal at δ_H 5.42 ppm was monitored. [f] The signal at δ_H 4.71 ppm was monitored. [g] The signal at δ_H 2.67 ppm was monitored.

In the case of the binary solvent mixture based on DMSO-d_6-D_2O (20% v/v) the situation is quite similar with an almost equivalent diffusion coefficient of 1.0 10^{-10} m^2 s^{-1}. Interestingly, in this polar and protic solvent media, the hydrodynamic radii difference is slightly increased (*ca*. 0.3 Å) and the overall size of both flavonoids significantly higher, probably due to some hydrogen bonding interaction with the solvent in parallel with some extent of aggregation in the binary mixture DMSO-d_6-D_2O.

Figure 2 illustrates the variation of the diffusion coefficients and hydrodynamic radii difference as a function of SDS concentration

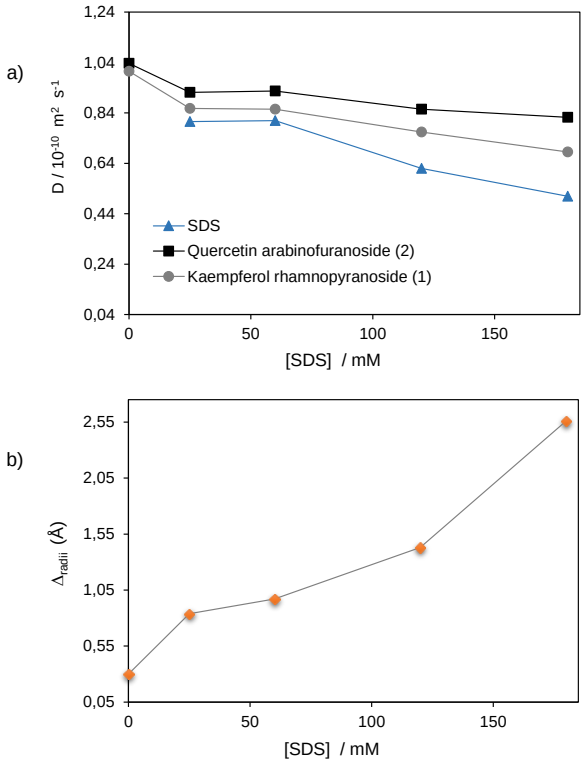

Figure 2. a) Diffusion coefficients as a function of SDS concentration for a DMSO-d_6-D_2O (20% v/v) solution containing flavonoid glycosides **1** and **2** in a 0.4:1.0 ratio, respectively. b) Hydrodynamic radii difference (Δr_H) berween **1** and **2** as a function of SDS concentration.

Increasing the SDS concentration leads to a significant decrease in diffusion coefficient for all the species present, while their differences more pronounced within the increased of SDS concentration.

The almost equal D-values obtained for DMSO and HDO in samples containing SDS and without it (entries 5-6 and 19-20, Table 3) validates the measurements performed under different conditions, and therefore explains why the increment in size is due to real interactions with the micelle and it is not ascribed to a change on viscosity. As expected, the maximum Δr_H (Figure 2b) between **1** and **2** was achieved when keeping the concentration of SDS well above the CMC at a concentration of 180 mM. The strongest association (i.e. the lowest diffusion coefficient) is seen for kaempferol rhamnopyranoside **1**, while the weakest is observed for quercetin arabinofuranoside **2** (Figure 3). Interestingly, the diffusion values of **1** and **2** in presence of 180 mM of SDS (entries 16 and 17, Table 3) is fully comparable with the D-value of the SDS micelle which shows that stable isotropic aggregates between **1** or **2** and the detergent are formed.

Figure 3 shows the scenario found well above the CMC at a concentration of SDS of 180 mM. In fact, the flavonoid derivatives **1** and **2** interact differentially with the micelles and as a result show different diffusion coefficients ($0.68\ 10^{-10}$ and $0.82\ 10^{-10}$ $m^2\ s^{-1}$. for **1** and **2**, respectively). Although there is some overlap of signals between compounds, they are sufficiently well resolved in the presence of SDS to allow adequate characterization.

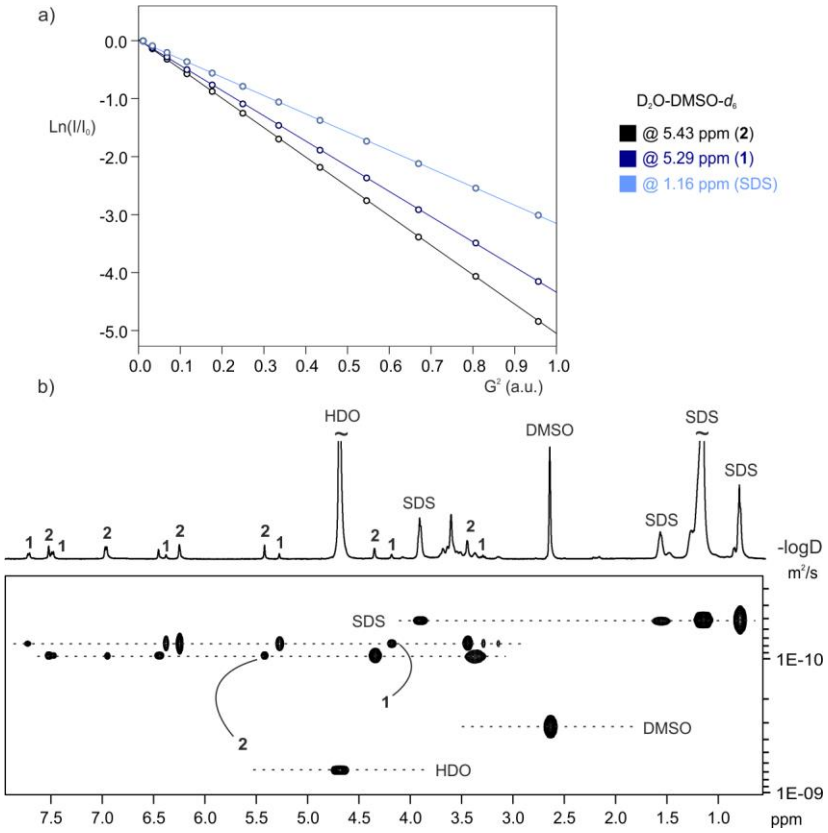

Figure 3. a) Linearized Stejskal−Tanner fit of the PGSE data and b) ^{1}H DOSY (500 MHz) spectrum with the least attenuated 1D spectrum on top, for **1** and **2** containing 180 mM of SDS in a binary mixture DMSO-d_6-D_2O (20% v/v).

The observation that addition of surfactant leads to DOSY resolution is of immediate practical significance, but it is clearly tempting to speculate of the mechanism of interaction. The retention of sharp lines for each solute (and for surfactant) indicates that the species remain in fast exchange, as is common for micellar solutions, with an equilibrium between free and associated states. A simple model for an aqueous system would be the incorporation of solutes into the micellar core, for which the partitioning of the glycoside between free and bound states will depend on hydrophobicity. However, the presence of several hydroxyl groups in compounds **1**

and **2** in a protic media suggest that this is at best a partial explanation, and other factors such as hydrogen-bonding interactions at the micelle core/headgroup interface, and π-stacking effects could enhance or weaken the binding to the micelles.

To shed light on the existing interactions that discriminate the two flavonoid glycosides in SDS-micelles we measured one-dimensional build-up NOESY curves in order to estimate inter-moiety distances between each of the two natural products and SDS-micelles.

NOESY studies. The use of selective 1D-NOESY (1D DPFGSE-NOE) pioneered by A. J. Shaka *et al*.[51] and later refined by Krishnamurthy *et al*.,[52] instead of 2D NOESY or steady-state NOE-experiments, enable an increased sensitivity per unit of data collection time and a better control on the baseline, In addition, the linearity of 1D-NOESY growing curves has been proven to be larger than in the 2D-NOESY experiment due to the dependency of the growing rate on T_1 selective.[52]

The determination of the inter-proton distances described herein is based on comparison of build-up NOESY rates for pairs of spins where we standardize the intensity of each NOE peak versus another intensity in the same selective inversion experiment.

We found in our experiments that there are negligible negative (relayed) NOESY peaks, and all relative NOE intensities are essentially constant with mixing time (up to ~1.0s), i.e. each NOE builds-up at a rate proportional to its initial intensity during this time.[53a] In general, the integral of each NOE signal is divided by the integral of the excited peak to produce the normalized build-up intensities that is used to calculate the NOE build-up rates(s) from the slope. Figure 4 shows one-dimensional NOESY spectra for the selective inversion of H-R1 (top) and

H-A1 (bottom), evidencing signal enhancement due to both inter- and intra-molecular dipolar interactions.

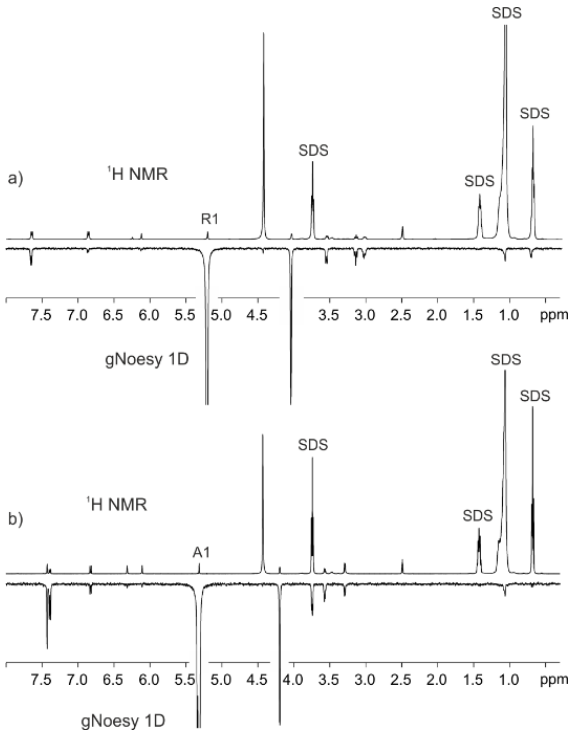

Figure 4. a) Comparison of the ^{1}H NMR spectrum of the kaempferol-3-O-rhamnopyranoside **1** and the 1D ^{1}H,^{1}H-DPFGSE NOESY spectrum (t_m 0.5 s) with selective excitation of the anomeric proton H-R1. b) Comparison of the ^{1}H NMR spectrum of the quercetin-3-O-arabinofuranoside **2** and the 1D ^{1}H,^{1}H-DPFGSE NOESY spectrum (t_m 0.5s) with selective excitation of the anomeric proton H-A1.

We have calculated herein the inter-protonic distances between SDS-micelles and the flavonoid glycosides by the -1/6 power of the cross-relaxation rates ratio between the unknown distance and that for a reference fixed distance times the reference distance. The respective

cross-relaxation rates, σ, were obtained by linear fitting of the normalized growing curves, using the excited peak intensity at the same mixing time to minimize relaxation bias.[53b] To do so, two new samples were prepared and analyzed, separately, containing each glycoside flavonoid and SDS up to a concentration of 180 mM in the same binary mixture DMSO-d_6-D_2O (20% v/v) employed in PGSE and MAD studies. In order to corroborate that under similar experimental conditions the same micellar media was created in both samples, we performed DLS experiments on a Malvern zetasizer instrument. We found that the hydrodynamic volume diameters for both samples to be 5.11 and 5.13 nm (see Supporting Information), that unequivocally shows reproducible micellar media in both situations. The selective 1D DPFGSE -NOESY spectrum of H-R1 and H-A1 show clear and well-resolved NOE enhancements with very flat baselines, which are representative of all of the spectra, obtained in this study. The analysis to determine inter-proton distances on both samples is illustrated in Figure 5. Selective 1D-NOESY (1D DPFGSE-NOE) were obtained over a range of mixing times, i.e. 100, 200, 300, 400, 500 and 1000 ms.[51,54]

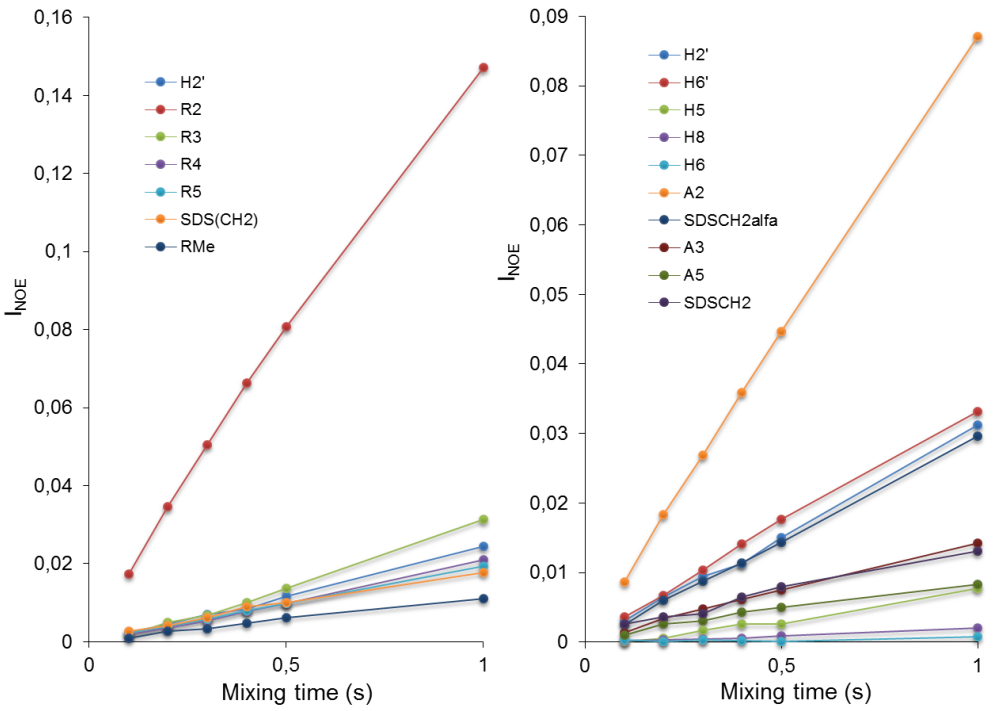

Figure 5. NOESY intensities (I_{NOE}) normalized with respect to the inverted peak intensity and plotted against mixing time (t_m). Left: Selective excitation of H-R1; Right: Selective excitation of H-A1.

The NOE intensities, normalized with respect to the inverted peak intensity, were plotted against the mixing time to obtain build-up rates that, to a large extent, canceled the effect of external relaxation at moderate mixing times.[52] The average interproton distances, were then calculated from the obtained cross-relaxation rates (σ values) and the intramolecular reference distance, assuming that the tumbling of the system can be described by a single rotational correlation time. The corresponding reference distance of 4.3 Å between meta protons H6 and H8 was derived from experimental data available from X-ray diffraction. For example, the cross-relaxation rate constants for the intramolecular H-R1/H-R2 and H-A1/and H-A2 were σ =

0.142801 s^{-1} and σ = 0.086681 s^{-1}, corresponding to estimated distances of ~3.36 and ~3.09 Å, respectively (Table 4).

Table 4. Cross relaxation rate constant (σ_{IS}, s^{-1})[a] and internuclear distance (r_{IS}, Å)[b] at a ^1H frequency of 500 MHz.

1	σ_{IS} (s^{-1})	r_{IS} (Å)	2	σ_{IS} (s^{-1})	r_{IS} (Å)
R1-SDS_{CH2}	0.008468	5.38	A1-SDS_{α}	0.014922	4.15
R2-SDS_{CH2}	0.009881	5.24	A1-SDS_{CH2}	0.006003	4.83
H8-SDS_{CH2}	0.013899	4.95	A2-SDS_{α}	0.041484	3.50
H2'-SDS_{CH2}	0.014883	4.90	A2-SDS_{CH2}	0.005693	4.87
H3'-SDS_{CH2}	0.010058	5.23	A5-SDS_{α}	0.004027	3.51
-	-	-	H8-SDS_{CH2}	0.0009245	4.49
R1-H2'	0.024653	4.50	A1-H2'	0.0311375	3.67
R2- H2'	0.058327	3.90	A1- H6'	0.0329140	3.63
R2-H3'	0.020418	4.65	A1-A2	0.086681	3.09
R1-R2	0.142801	3.36	A1-A3	0.0140340	4.19
H8-H2'	0.023118	4.55	A5-H2'	0.0130481	4.24
H8- H6’	0.032537	4.30	A5-H6’	0.0153984	4.12
H2'-H3'	0.406921	2.82	H8-H2'	0.0160719	4.09
-	-	-	H8- H6'	0.0117785	4.31
-	-	-	H5'-H6'	0.2495815	2.59

[a] All the fits have R^2 values higher than 0.99 and the estimated error for a single σ_{IS} value is about 10%. [b] Reference distance of 4.3 Å between meta protons H6 and H8 was used for both **1** and **2**.

In the case of the more interesting intermolecular interactions, the cross-relaxation rate constants for H-R1/H-SDS_{CH2} and H-A1/H-SDS_{α} were $\sigma = 0.008468\ s^{-1}$ and $\sigma = 0.014922\ s^{-1}$, corresponding to estimated distances of ~5.38 and ~4.15 Å, respectively. The estimations of the average cross relaxation rate constants and the distances derived from the whole analysis are shown in Table 4.

Together with the quantitative analysis described above, we performed a qualitative examination of the two-dimensional NOESY performed on samples constituted *ex professo* as mentioned above. Under these experimental conditions, the corresponding integration of the cross-peaks provided us with an intensity map for the interaction of each natural product with the SDS micelle. Considering only the strongest (red in Table 5) and medium to strongest intensity interactions (orange in Table 5), it is remarkable that only the kaempferol derivative interacts with the methyl group of the SDS micelles, exhibiting a clear insertion of the product into the inner part of the micelle. On the other hand, the quercetin derivative only gives NOE interactions with the alpha and internal methylene groups, describing a picture where the natural product is not so deeply inserted into the micelle which placed it somehow closer to the surface of the SDS-micelle (see Table 5 and Supporting Information for full intensity NOESY maps).

Table 5. Strong- and medium-intensity NOE cross-peaks derived from 2D gNOESY at 500 MHz and 0.5 s of mixing time, between the two flavonoid glycosides **1** and **2** and the SDS-micelle at 180 mM in a binary mixture solvent based on DMSO-d_6-D_2O (20% v/v).

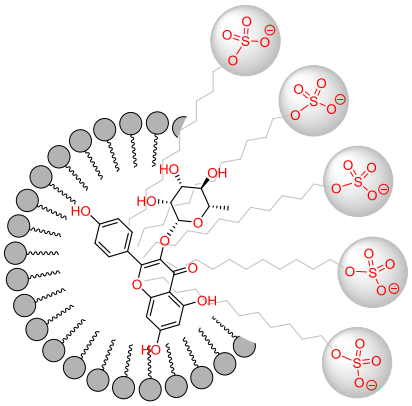

Kaempferol-3-O--α-L-rhamnopyranoside

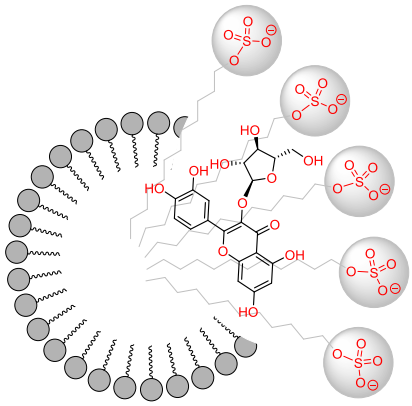

Quercetin-3-O-α-L-arabinofuranoside

1	SDS_{Me}	SDS_{CH2}	SDS_{α}	**2**	SDS_{Me}	SDS_{CH2}	SDS_{α}
R1	-	■		A1		■	-
R4	■	-		A2		-	■
R5	■	-		A3		■	■
H3’	-	■		A4		■	-
H6	-	■		A5		■	■
H8	-	■		H5’		■	-
				H6’		-	-
				H8		■	-

[a] All the fits have R^2 values higher than 0.99 and the estimated error for a single σ_{IS} value is about 10%. [b] The reference distance used was H6-H8 for both **1** and **2**.

To summarize, the two flavonoid glycosides under study, **1** and **2**, were analyzed using a systematic *in silico* M06 functional computational study (with an ultrafine grid) with the aim of understanding the molecular factors that determine their interaction with SDS micelles.

Optimizations were carried out in water solvent using the continuum method SMD, where no explicit water molecules were explicitly computed. Compounds **1** and **2** were optimized in the presence of one and two hexylsulfate molecules (used as a model molecules for SDS) in water solvent. Unfortunately, the consideration of isolated surfactant molecules was too simplistic to reproduce the micellar environment properly. The results were not conclusive since similar energies and interactions were found for both species (see Supporting Information). More advanced models are required to reproduce the hydrophilic and hydrophobic interaction between **1** and **2** and the micelle. These simulations are however beyond the scope of the present study.

In conclusion, two compounds, kaempferol-3-O-α-L-rhamnopyranoside (**1**) and quercetin-3-O-α-L-arabinofuranoside (**2**), have been isolated for the first time from leaves of *Persea caerulea*. Their structures have been fully characterized by ^{1}H NMR, ^{13}C NMR and IR spectrocopy, together with LC coupled to different MS analyzers (TOF and IT MS). The information from MS was crucial to determine the molecular weights of the intact molecules as well as those of quercetin and kaempferol together with their sugar moieties have been deduced. Matrix-assisted DOSY and PGSE have been applied, using a binary solvent mixture and SDS micelles as a function of concentration, to exploit differential binding to separate the NMR signals of both compounds. Investigations of the nature of the interactions between glycosides **1** and **2** and SDS micelles have been conducted by accurately measuring of inter-proton distances using selective 1D ^{1}H,^{1}H NOESY. The calculated average distances derived from the obtained σ values and the intramolecular reference distance showed a clear insertion of the kaempferol derivative **1** into the inner part of the micelle, whereas the quercetin analog **2** only gives interactions with the alpha and internal methylene groups, describing a picture where the natural

product is placed closer to the surface of the SDS-micelle. Together with the quantitative analysis, a qualitative examination of two-dimensional NOESYs confirmed selective interactions and therefore different solution dispositions within the micelle.

EXPERIMENTAL SECTION

General procedures. Infrared spectra were recorded in a Bruker Alpha FTIR spectrophotometer. Me_2CO-d_6, DMSO-d_6 and heavy water were purchased from Eurisotop. All other reagents and solvents were of commercial quality and were used without further purification. NMR spectra were measured on a Bruker Avance III 300 (^{1}H, 300.13 MHz; ^{13}C, 75.47 MHz) and a Bruker Avance III 500 spectrometer equipped with a third radiofrequency channel (^{1}H, 500.13 MHz; ^{13}C, 125.76 MHz) using a 5 mm BBFO ^{1}H/BB(^{19}F) probe and an indirect 5 mm TBI ^{1}H/^{31}P/BB triple probe, respectively. Unless otherwise stated, standard Bruker software routines (TOPSPIN) were used for the 1D and 2D NMR measurements. Chemical shifts are given in ppm for TMS for ^{13}C and ^{1}H. Coupling constants, *J*, are given in Hertz as positive values regardless of their real individual signs. Stock solutions of the flavonoids in DMSO-d_6 were diluted either with D_2O or D_2O and a solution of SDS in D_2O, as appropriate, to yield a final concentration of 25 mM for each flavonoid. The sample selected for MAD experiments was prepared by using the corresponding fraction containing the two flavonoids glycosides under study, and adding SDS to progressively yield a final concentration of 25, 60, 120 and 180 mM. Dynamic light scattering (DLS) data were acquired using a Malvern Zetasizer Instrument, equipped with a 4 mW He-Ne 633 nm laser module at 25 ºC. Measurements were carried out at a detector angle of 173º (back scattering) and the resulting data analyzed by the Malvern DTS 7.03 software.

Plant Material. The leaves of *P. caerulea* were collected in the town of San Pedro de la Sierra, Magdalena department, Colombia, over December 2009. The Plant material was identified by the botanist Adolfo Jara. A voucher specimen (COL 518189) was deposited at Herbario Nacional Colombiano, Natural Sciences Institute, Universidad Nacional de Colombia.

Extraction and isolation. Silica gel (230-400 mesh, Merck) was used for flash chromatography (FC), silica gel 60 F_{254} chromatoplates Merck, for TLC and vacuum liquid chromatography (VLC) was carried out with silica gel 60 (70-230 mesh) Merck. Air-dried and powdered leaves of *P. caerulea* (2175 g) were exhaustively extracted with 96% ethanol by maceration at room temperature. The solvent was evaporated under vacuum to yield 345.8 g of the crude extract. A sample of this extract (58 g) was fractionated by VLC on silica gel using ether petroleum, toluene, chloroform, ethyl acetate and methanol as mobile phase producing 5 fractions. The ethyl acetate fraction (25 g) was subjected to flash chromatography (FC) on silica gel, eluted with a mixture of toluene-isopropyl acetate at increasing polarity (from 7:3 to 5:5), to yield 22 fractions. Fraction 15 (350 mg) was purified again by FC and eluted with toluene-ethyl acetate-acetic acid (6: 4: 1) to afford 10 mg of a mixture of **1** and **2**.

LC-MS instruments. Two different LC-MS platforms were used in the current study. The first one was an Agilent 1260 LC system (Agilent Technologies, Waldbronn, Germany) equipped with a diode-array detector (DAD) coupled to a Bruker Daltonic Esquire 2000™ ion trap mass spectometer (Bruker Daltonik, Bremen, Germany) with an electrospray ionization (ESI) interface. The second one was a Waters Acquity UPLC™ H–Class system (Waters, Manchester, UK) coupled to a microTOF mass spectrometer (Bruker Daltonik) equipped with an electrospray source as well. The first one was mainly used to get MS/MS signals (and to study the fragmentation of the analytes under study) and the second one was used to achieve accurate

MS data which was very important to get an unequivocal identification. The accurate mass data of the molecular ions were processed as reported previously.[55] Internal calibration was performed using sodium formate cluster with a solution containing 5 mM of sodium hydroxide in the sheath liquid of 0.2% formic acid in water/isopropanol 1:1 v/v. The calibration solution was injected at the beginning of the run and all the spectra were calibrated prior carrying out the compound identification.

LC-MS conditions. In both cases, the compounds under study were separated by using an Eclipse Plus analytical column (4.6 x 150 mm, 1.8 μm particle size) (Agilent Technologies), operating at 25ºC. The mobile phases were water with 0.5% of acetic acid (Phase A) and acetonitrile (Phase B). Analytes were eluted at a flow rate of 0.8 mL/min according to the following gradient: from 95% A to 0% A in 30 min, returning to the initial conditions and equilibrating the column for 1.5 min. The injection volume was 10 μL. The mass spectrometric conditions were optimized for both compound by continuous infusion of standard solutions (at a concentration level of 2 mg/L approx.). The end plate offset voltage was set at -500 V, and the capillary voltage at +3200 V in negative polarity, and -4000 V when positive polarity was used. Optimum values for the ESI source parameters were: 300ºC of drying gas temperature, 9 L/min of drying gas flow and 30 psi of nebulizer pressure. These parameters were then transferred to the ESI-TOF spectrometer.

Diffusion experiments. PGSE NMR diffusion measurements were carried out using the stimulated echo sequence and bipolar pair pulses.[56] A sine shape was used for the gradient pulses and their strength varied automatically in the course of the experiments. The D values were determined from the slope of the regression line $\ln(I/I_0)$ versus G^2, according to the Stejskal-Tanner equation for sine bell shaped gradient pulses (equation 1)[57] and employing the

DiffAtOnce package.[58] I/I_0 = observed spin echo intensity/intensity without gradients, G = gradient strength, Δ = delay between the midpoints of the gradients, D = diffusion coefficient, δ = gradient length.

$$\ln(\frac{I}{I_0}) = -(\gamma\delta)^2(\Delta - \frac{\delta}{4})D\frac{4}{\pi^2}G^2 \qquad (1)$$

The measurements were carried out without spinning. Gradient calibration was carried out by means of a diffusion measurement of HDO in D_2O (D(HDO) = 1.902 x 10^{-9} m^2 s^{-1}).[59] To check reproducibility, three different measurements with different diffusion parameters (δ and/or Δ) were always carried out. The experimental error in D values was estimated to be smaller than ±2%. All of the data leading to the reported D values afforded lines whose correlation coefficients were above 0.999. The gradient strength was incremented in 4–8% steps from 2–10% to 98% so that, depending on signal:noise, 12–25 points could be used for regression analysis. The recovery delay was set to 5 s. DOSY NMR data were acquired using the Oneshot[60] pulse sequence with a total diffusion encoding pulse duration δ of 2-4 ms, a diffusion delay Δ of 100-200 ms, and 12-24 nominal gradient amplitudes ranging from 5 to 95% of G to give equal steps in gradient squared. Experiments were carried out without active temperature regulation, at the probe ambient temperature of 25 ± 1 °C. DOSY spectra were constructed by standard methods,[61] using fitting to a modified Stejskal-Tanner equation parameterized to take into account the effects of pulsed field gradient non-uniformity. DOSY spectra were processed and evaluated by using the exponential fit implemented in Topspin 2.0. The diffusion dimension was zero-filled to 1K, sine window function with line broadening of 0.5 Hz and sine bell shift equal to zero. This dimension was exponentially fitted according to a preset window (log D = −12.0 to −8.0). Gaussian line shapes were chosen to optimize the resolution of neighboring signals in F2 and no reference deconvolution was used.

NOESY experiments. Selective 1D DPFGSE NOE experiments were carried out by using the double pulse field gradient echo sequence[51] with different mixing times varying from 0.1 to 1.0 s. The data were collected using a spectral width of 5000 Hz and 16384 complex data points for a 1.64 s acquisition time with a 1 s recycle delay. Selective Gaussian pulses of 20 ms were used to invert the target resonances. Processing of the spectra was accomplished by zero filling to 64 K followed by an exponential multiplication using a line width of 1 Hz. All NOESY peaks areas were subsequently divided by the area of the inverted signal at the same mixing time. This ensures that the enhancements are corrected for relaxation effects. Inter-proton distances were obtained from the slopes of the normalized growing rates versus mixing time obtained by linear regression, and applying the isolated spin pair approach (ISPA) using the rigid H6-H8 distance as reference and the peak at the same mixing time to account for relaxation effects. All the distances were calculated from σ ratios by including the appropriate correction factors to account for the number of protons involved, i.e. those involving SDS_{CH2}, the σ_{IS} was calculated dividing the slope of the normalized growing rate by a factor of two. All the fits have R^2 values higher than 0.99 and the estimated error for a single σ_{IS} value was about 10%. 2D NOESY spectra were collected with 0.5 seconds of mixing time using a spectral width of 7508 Hz in F2 and 2048 complex data points for an acquisition time of 0.136 s with a 2 s recycle delay. 256 points were collected in the indirect F1 dimension for a 0.025 s acquisition time. 80 scans were collected per F1 increment and F1 quadrature detection was achieved using the States-TPPI method. Time domain data were apodized using squared sine bell functions in both dimensions and zero-filled in the indirect dimension to a final data matrix size of 1024 (F1) x 2048 (F2) after Fourier transformation.

Supporting Information. NMR and MS full structural characterization, comparison of our NMR data with literature data sets, DLS measurements, NOESY maps and DFT optimized structures and energies. This material is available free of charge via the Internet at http://pubs.acs.org.

ACKNOWLEDGMENTS

This work was supported by the Junta de Andalucía (Spain) under the project number P12-FQM-2668. I.F and the División de Investigación Sede Bogotá (DIB) (project code No 15220) at Universidad Nacional de Colombia thank the Spanish specialized group of NMR (GERMN) for a travel grant. We are grateful to Dr. Manuel A. Ortuño (University of Minnesota) for the performing DFT calculations and Prof. Agustí Lledós and Prof. Gregori Ujaque (Universitat Autònoma de Barcelona) for generous allocation of computer time.

REFERENCES

1 M. López-Lázaro, J. Calderón-Montaño, E. Burgos-Morón, C. Pérez-Guerrero, *Mini-Reviews in Medicinal Chemistry,* **2011***, 11,* 298-344.

2 R. March, E. Lewars, C. Stadey, X. Miao, X. Zhao, C. Metcalfe, *Int. J. Mass Spectrom.* **2006**. *248*, 61–85.

3 M. Berhow, F. Vaughn, *Higher plant flavonoids: Biosynthesis and chemical ecology*. In Principles and Practices in Plant Ecology. Allelochemical Interaction; K. Dakshini, C. Foy, Eds.; CRC Press LLC: Florida, FL, USA, 1999; pp. 423–438.

4 R. Dixon, M. Harrison, C. Lamb, *Annu. Rev. Phytopatol*. **1994**. *32*, 479-501.

5 H. Spaink, *Annu. Rev. Phytopatol*. **1995**. *33*, 345-368.

6 V. Gianinazzi-Pearson, *Plant Cell*. **1996**. *8*, 1871-1883.

7 J. B. Harborne, C. A. Williams, *Phytochemistry*, **2000**, *55*, 481–504.

8 S. Granica, A. Kiss, *Biochem. Syst. Ecol*., **2012**, 44-47.

9 H. Wangensteen, C. Nergard, B. Paulsen, D. Diallo, K. Malterud, N. Tran-Le, *J. Ethnopharmacol*. **2012**. *139*, 858– 862.

10 I. Vedenskaya, N. Vorsa, *Plant Science*. **2004**, *167*, 1043–1054.

11 A. Almeida, M. Miranda, I. Simoni, M. Wigg, M. Lagrota, S. Costa, *Phytomedicine*. **1997**, *4*, 347-352.

12 A. Almeida, M. Miranda, I. Simoni, M. Wigg, M. Lagrota, S. Costa, *Phytotherapy. Res*. **1998**, *12*, 562-567.

13 V. Vo, J. Lee, J. Chang, J. Kim, N. Kim, H. Lee, S. Kim, W. Chun, K. Yong-Soo, *Biomol. Ther.* **2012**, *20*, 532-537.

14 F. Cuyckens, M. Claeys, *J. Mass Spectrom.* **2004**, *39*, 1–15.

15 M. Stobiecki, *Phytochemistry* **2000**, *54*, 237-256.

16 S. Lavoie, C. Gauthier, V. Mshvildadze, J. Legault, B. Roger, A. Pichette, *J. Nat. Prod*. **2015**, DOI: 10.1021/acs.jnatprod.5b00492.

17 J. Cassani, M. Nilsson, G. A. Morris, *J. Nat. Prod.* **2012**, *75*, 131-134.

18 T. Fossen, Ø. M. Andersen, *Spectroscopic Techniques Applied to Flavonoids in: Flavonoids – Chemistry, Biochemistry and Applications*, Ø. M. Andersen, K. R. Markham, Eds. Taylor & Francis, 2005; pp 37-142.

19 J. B. Harborne, T. J. Mabry, *The flavonoids: Advances in research.* In C-13 NMR Spectroscopy of Flavonoids, K. R. Markham, V. Mohanchari, Eds., Chapman & Hall Ltd: University Press: Cambridge, London, UK, 1982; pp. 119-132.

20 K.-R. Markham, B. Temai, R. Stanley, H. Geiger, T.-J. Mabry, *Tetrahedron* **1978**, *34*, 1389-1397.

21 a) L. L. Saldanha, W. Vilegas, A. L. Dokkedal, *Molecules*, **2013**, *18*, 8402-8416. b) A. Lommen, M. Godejohann, D. P. Venema, P. C. H. Hollman, M. Spraul, *Anal. Chem*. **2000**, *72*, 1793-1797.

22 M. Olszewska, M. Wolbis, *Acta Pol. Pharm*. **2001**, *58*, 367-372.

23 a) P.-H. Wang, S.-S. Lee, *J. Chin. Chem. Soc*. **1999**, *46*, 215-219. b) S.-H. Lam, C.-K. Chen, J.-S. Wang, S.-S. Lee, *J. Chin. Chem. Soc*. **2008**, *55*, 449-455.

24 C.-J. Shen, C.-K. Chen, S.-S. Lee, *J. Chin. Chem. Soc.* **2009**, *56*, 1002-1009.

25 M. Kalegari, M. D. Migue, J. F. G. Dias, A. L. L. Lordello, C. P. Lima, C. M. S. Miyazaki, S. M. W. Zanin, M. C. S. Verdam, O. G. Miguel, *Braz. J. Pharm. Sci*. **2011**, *47*, 635–42.

26 D. Sohretoglu, M. K. Sakar, S. A. Sabuncuoglu, H. Ozgunes, O. Sterner, *Turk. J. Chem*. **2009**, *33*, 685-692.

27 J.-X. Liu, D.-L. Di, Y.-P. Shi, *J. Chin. Chem. Soc*. **2008**, *55*, 863-870.

28 M. A. Lhuillier, Ph.D. Thesis, L'institut National Polytechnique de Toulouse, 2007.

29 V. Vukis, *Mass Spectrom. Rev.* **2010**, *29*, 1-16.

30 Q. Li, M. Claeys, *Biol. Mass Spectrom.* **1994**, *23*, 406–416.

31 R. Llorach, A. Gil-Izquierdo, F. Ferreres, F. Tomas-Barbera, *J. Agric. Food Chem.* **2003**, *51*, 3895–3899.

32 (a) E. O. Stejskal, J. E. Tanner, *J. Chem. Phys*. **1965**, *42*, 288−292. (b) B. Antalek, *Concepts Magn. Reson*. **2002**, *14*, 225−258.

33 C. S. Jr. Johnson, *J. Magn. Reson. A* **1993**, *102*, 214-218.

34 S. Viel, F. Ziarelli, S. Caldarelli, *Proc. Natl. Acad. Sci. USA* **2003**, *100*, 9696–9698; b) G. Pages, C. Delaurent, S. Caldarelli, *Anal. Chem*. **2006**, *78*, 561–566.

35 K. F. Morris, P. Stilbs, C. S. Jr. Johnson, *Anal. Chem*. **1994**, *66*, 211–215.

36 S. Viel, F. Ziarelli, S. Caldarelli, *Proc. Natl. Acad. Sci. U.S.A*. **2003**, *100*, 9696-9698.

37 R. Evans, S. Haiber, M. Nilsson, G. A. Morris, *Anal. Chem*. **2009**, *81*, 4548-4550.

38 C. F. Tormena, R. Evans, S. Haiber, M. Nilsson, G. A. Morris, *Magn. Reson. Chem*. **2010**, *48*, 550-553.

39 C. F. Tormena, R. Evans, S. Haiber, M. Nilsson, G. A. Morris, *Magn. Reson. Chem*. **2012**, *50*, 458-465.

40 J. S. Kavakka, I. Kilpelainen, S. Heikkinen, *Org. Lett*. **2009**, *11*, 1349-1352.

41 J. S. Kavakka, V. Parviainen, K. Wahala, I. Kilpelainen, S. Heikkinen, *Magn. Reson. Chem*. **2010**, *48*, 777-781.

42 R. E. Hoffman, H. Arzuan, C. Pemberton, A. Aserin, N. J. Garti, *Magn*. *Reson*. **2008**, *194*, 295-299.

43 R. W. Adams, J. A. Aguilar, J. Cassani, G. A. Morris, M. Nilsson, *Org. Biomol. Chem*. **2011**, *9*, 7062.

44 M. G. S. Vieira, N. V. Gramosa, N. M. P. S. Ricardo, G. A. Morris, R. W. Adams, M. Nilsson, *RSC Adv*. **2014**, *4*, 42029-42034.

45 a) C. Pemberton, R. E. Hoffman, A. Aserin, N. Garti, *Langmuir* **2011**, *27*, 4497-4504; b) R. E. Hoffman, A. Aserin, N. Garti, *Magn. Reson*. **2012**, *220*, 18-25.

46 a) P. C. Hiemenz, R. Rajagopalan, *Principles of Colloid and Surface Chemistry*, 3rd ed; Marcel Dekker: New York, 1997; pp 331-338. b) D. F. Evans, H. Wennerström, *The Colloidal Domain;* VCH: New York, 1994; Chapter 3.

47 S. A. Markarian, L. R. Harutyunyan, R. S. Harutyunyan, *J. Solution Chem.* **2005**, *34*, 361−368.

48 R. E. Hoffman, E. Darmon, A. Aserin, N. Garti, *J. Colloid Interface. Sci*. **2016**, *463*, 358-366.

49 $D = kT/(6\pi\eta r_H)$, where r_H is the hydrodynamic radius, D the diffusion coefficient, k the Boltzmann constant, T the absolute temperature and η the solvent viscosity.

50 a) A. Macchioni, G. Ciancaleoni, C. Zuccaccia, D. Zuccaccia, *Chem. Soc. Rev.* **2008**, *37*, 479; b) R. Evans, Z. Deng, A. K. Rogerson, A. S. McLachlan, J. J. Richards, M. Nilsson, G. A. Morris, *Angew. Chem. Int. Ed.* **2013**, *52*, 3199.

51 a) K. Stott, J. Stonehouse, J. Keeler, T.-L. Hwang, J. Shaka, *J. Am. Chem. Soc.* **1995**, *117*, 4199. b) K. Stott, J. Keeler, Q. N. Van, A. J. Shaka, *J. Magn. Reson*. **1997**, *125*, 302–324.

52 H. Hu, K. Krishnamurthy, *J. Magn. Reson*. **2006**, *182*, 173-177.

53 For a detailed explanation of this methodology for intra- and inter-residue distance determination see: a) S. Macura, R. R. Ernst, *Mol. Phys*. **1980**, *41*, 95–117; b) S. Macura, B. T. Farmer, L. R. Brown, *J. Magn. Reson*. **1986**, *70*, 493-499.

54 a) J. Stonehouse, P. Adel, J. Keeler, J. Shaka, *J. Am. Chem. Soc*. **1994**, *116*, 6037. b) D. J. McCord, J. H. Small, J. Greaves, Q. N. Van, A. J. Shaka, E. B. Fleischer, K. J. Shea, *J. Am. Chem. Soc*. **1998**, *120*, 9763.

55 R. García-Villalba, C. León, G. Dinelli, A. Segura-Carretero, A. Fernández-Gutiérrez, V-García-Cañas, A. Cifuentes, *J. Chromatrogr. A*. **2008**, *1195*, 164-173.

56 D. H. Wu, A. D. Chen, C. S. Johnson, *J. Magn. Reson. Ser., A* **1995**, *115*, 260.

57 D. Sinnaeve, *Concepts Magn. Reson*. **2012**, *40A*, 39-65.

58 DiffAtOnce is a registered program developed by Fernández, I. and Arrabal-Campos, F. M. in the University of Almería. 2013.

59 H. J. V. Tyrrell and K. R. Harris, *Diffusion in Liquids*, Butterworths, London, 1984.

60 M. D. Pelta, G. A. Morris, M. J. Stchedroff, S. J. Hammond, *Magn. Reson. Chem.* **2002**, *40*, S147-S152.

61 (a) C. S. Jr. Johnson, *Prog. Nucl. Magn. Reson. Spectrosc*. **1999**, *34*, 203–256. (b) G. A. Morris, In *Encyclopedia of Nuclear Magnetic Resonance*; D. M. Grant, R. K. Harris, Eds.; John Wiley & Sons Ltd: Chichester, 2002; Vol. 9: Advances in NMR, pp 35-44.

Insert Table of Contents Graphic and Synopsis Here

Two compounds, kaempferol-3-O-rhamnopyranoside (**1**) and quercetin-3-O-arabinofuranoside (**2**), have been isolated for the first time from leaves of *Persea caerulea*. Matrix Assisted DOSY and PGSE have been applied to exploit differential binding to separate the NMR signals. Calculated average inter-proton distances derived from 1D NOESY σ values revealed a differential insertion of both flavonoid glycosides into the micelles.

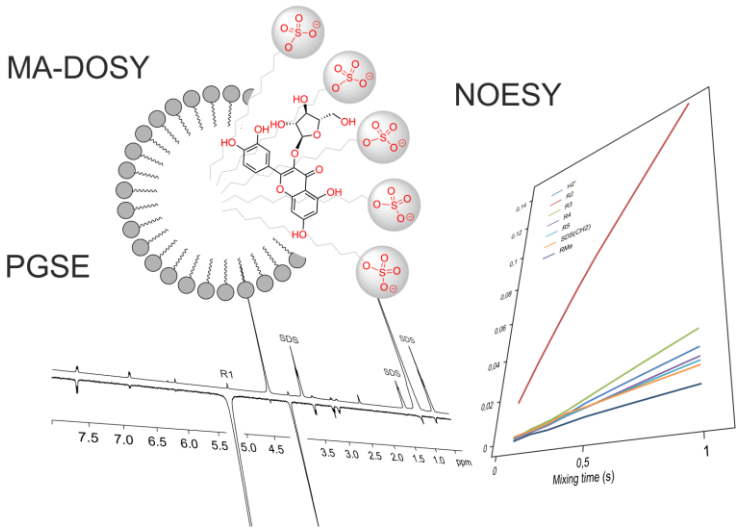
MA-DOSY
PGSE
NOESY
SDS
SDS
SDS
R1
7.5 7.0 6.5 6.0 5.5 5.0 4.5
3.5 3.0 2.5 2.0 1.5 1.0 ppm
0,5
1
Mixing time (s)